

# Effect of annealing on the structure and magnetic properties of mechanically milled $\text{TiO}_2\text{--Fe}_2\text{O}_3$ mixture

A.M. Al-Saie<sup>a,b</sup>, A. Al-Shater<sup>c,\*</sup>, S. Arekat<sup>a</sup>, A. Jaffar<sup>a</sup>, M. Bououdina<sup>a,b</sup>

<sup>a</sup>Department of Physics, University of Bahrain, P.O. Box 32038, Kingdom of Bahrain

<sup>b</sup>The Centre of Nanotechnology and Applied Research, University of Bahrain, Central Laboratories, P. O. Box 32038, Kingdom of Bahrain

<sup>c</sup>Centre for Engineering and Technology Studies, University of Bahrain, P.O. Box 32038, Kingdom of Bahrain

Received 17 September 2012; received in revised form 16 October 2012; accepted 17 October 2012

Available online 8 November 2012

## Abstract

A mixture of  $\text{Fe}_2\text{O}_3$  and  $\text{TiO}_2$  oxides has been mechanically milled to form  $\text{TiFe}_2\text{O}_4$  spinel phase. X-ray diffraction (XRD) pattern of the as-milled mixture shows the presence of both  $\text{Fe}_2\text{O}_3$  and  $\text{TiO}_2$  phases. The diffraction peaks become broader and their relative intensity drastically decreases due to the particle size reduction and accumulation of strains. The milled powder was then subjected to annealing at different temperatures (600, 750, 900, 1200 °C). Annealing at 600 °C and 750 °C does not show any significant change in the phase formation. Nonetheless, XRD patterns show a narrowing and an increase in the intensity of  $\text{Fe}_2\text{O}_3$  peaks with respect to  $\text{TiO}_2$ , which was reflected by an evolution in particle nano-structure following SEM analysis. An increase in the intensity ratio of the major peaks belonging to  $\text{Fe}_2\text{O}_3$  relative to the as-milled mixture, which was associated with a reduction of the amount of  $\text{TiO}_2$ , suggested a possible insertion of Ti into the  $\text{Fe}_2\text{O}_3$  crystal lattice. However, in VSM measurements, annealing at 600 °C and 750 °C does not change the ferromagnetic phase but the effect of annealing was a notable reduction in the values of both  $M_s$  and  $M_r$  (saturation magnetization and remanence magnetization respectively). Ultimately, as the powder was heated to 900 °C a new phase seemed to have emerged, this phase was confirmed by SEM, XRD, and magnetic measurements (VSM) where it change phase from ferromagnetic to paramagnetic phase.

© 2012 Elsevier Ltd and Techna Group S.r.l. All rights reserved.

**Keywords:**  $\text{TiO}_2\text{--Fe}_2\text{O}_3$ ; Milling; XRD; Magnetic

## 1. Introduction

By virtue of the rapid development in nanoparticle technology, it has found wide deployment in areas such as industry, environmental protection and medical treatment with promising new applications constantly on the increase [1,2]. Because it has not only the characters of general nanoparticles, but also the advantages of good biologic compatibility, better photocatalytic activity, non-toxicity, stable medical performance, easy preparation, and is available at a reasonably low cost,  $\text{TiO}_2$  (NPs) are an excellent biomaterial. This rapidly leads to the development of a new field of research and technology called

spintronics. Spinel ferrites  $\text{MFe}_2\text{O}_4$  are very important magnetic materials that show great potential for many important technological applications such as information storage media, medical diagnostics, drug delivery, and sensors. Wide gap oxide diluted magnetic semiconductors (DMS) combine their electrical conductivity with ferromagnetism and optical transparency, thereby opening up the possibilities of new device concepts. Transition metal-doped  $\text{TiO}_2$ ,  $\text{SnO}_2$ , and  $\text{ZnO}$  belong to these classes of materials [3,4]. Gracia et al. [5] have prepared transparent  $\text{Fe/TiO}_2$  thin films with different Fe/Ti atomic ratios by ion beam-induced chemical vapor deposition. The as-prepared samples were amorphous but after the films are heated, a crystalline structure starts to appear between pure  $\text{TiO}_2$  and  $\text{Fe/TiO}_2$ , depending on the iron content [5]. Pal et al. [6] show that sintering binary mixed oxides of  $\text{TiO}_2/\text{Fe}_2\text{O}_3$  prepared by sol-gel method at 700 °C and

\*Corresponding author. Tel.: +973 17876883, Mob.: +973 39056021; fax: +973 17449148.

E-mail address: [abdulla.alshater@gmail.com](mailto:abdulla.alshater@gmail.com) (A. Al-Shater).

900 °C consist of very sharp peaks of pure rutile and pseudobrookite phases with the complete disappearance of anatase phase. Moreover, Kundu et al. [7] study the mechanism growth of nanoscale  $\alpha$ -Fe<sub>2</sub>O<sub>3</sub> embedded into TiO<sub>2</sub> matrix by the sol-gel technique. The authors show the presence of anatase phase of TiO<sub>2</sub> and as the sample is heated, the rutile phase of TiO<sub>2</sub> and  $\alpha$ -Fe<sub>2</sub>O<sub>3</sub> start to appear at high temperatures. He et al. [8] prepare Fe<sub>3</sub>O<sub>4</sub>-TiO<sub>2</sub> core-shell superparamagnetism nanoparticles using homogeneous precipitation method.

It is known that ball milling is a synthesis technique that currently attracts scientists as an alternative method of producing nanocrystalline materials [9,10]. In the present paper, the structure and magnetic properties evolution of Fe<sub>2</sub>O<sub>3</sub> and TiO<sub>2</sub> oxides mixture prepared by mechanical milling followed by subsequent annealing were investigated.

## 2. Experimental procedure

### 2.1. Sample preparation and annealing

High purity oxide reactants  $\alpha$ -Fe<sub>2</sub>O<sub>3</sub> and TiO<sub>2</sub> used in this work were provided by Aldrich. Mechanical milling was carried out using a Fritsch Pulverisette P6 unit under air for carefully weighed mixtures of oxide powder precursors. Particular consideration was given to parameters affecting milling intensity such as balls/powder ratio, balls diameter, milling speed, and duration. Consequently in this study, a balls/powder ratio of 20, a milling speed and time of 300 rpm and 20 h were adopted, respectively. The resultant as-milled oxides mixture was then annealed under air using a muffle furnace for 1 h at each of the following temperatures 600 °C, 750 °C, 900 °C, and 1200 °C.

### 2.2. Characterizations

Powder X-ray diffraction (XRD) measurements were carried out using a Phillips diffractometer equipped with Cu-K $\alpha$  radiation (1.54056 angstroms). The crystallite size (CS) and the microstrain (MS) were estimated using peak profile analysis with a software provided with the diffractometer, where the full width at half maximum (FWHM) is determined and then used for the calculation by introducing a standard value for instrument contribution to the peak broadening.

Magnetic measurements were performed at room temperature using PMC MicroMag 3900 model Vibrating Sample Magnetometer (VSM) having a 1T magnet.

A Ziess scanning electron microscope (SEM) was used to generate high magnification nanographs of the annealed nanoparticles to examine the structural changes with annealing.

## 3. Results and discussion

### 3.1. Microstructure evolution

A mixture of TiO<sub>2</sub> and Fe<sub>2</sub>O<sub>3</sub> oxides has been mechanically milled in order to form a TiFe<sub>2</sub>O<sub>4</sub> spinel phase which was then exposed to a sequence of annealing treatments at various temperatures. Fig. 1 shows scanning electron microscope (SEM) nanographs of the as-milled and subsequently annealed oxide mixture. In general it can be seen that as the annealing temperature increases the nanoparticles show an average increase in their size, this might be depicted by comparing Fig. 1b with Fig. 1d of the same scale. Comparing Fig. 1(a,b) for as-milled powder and

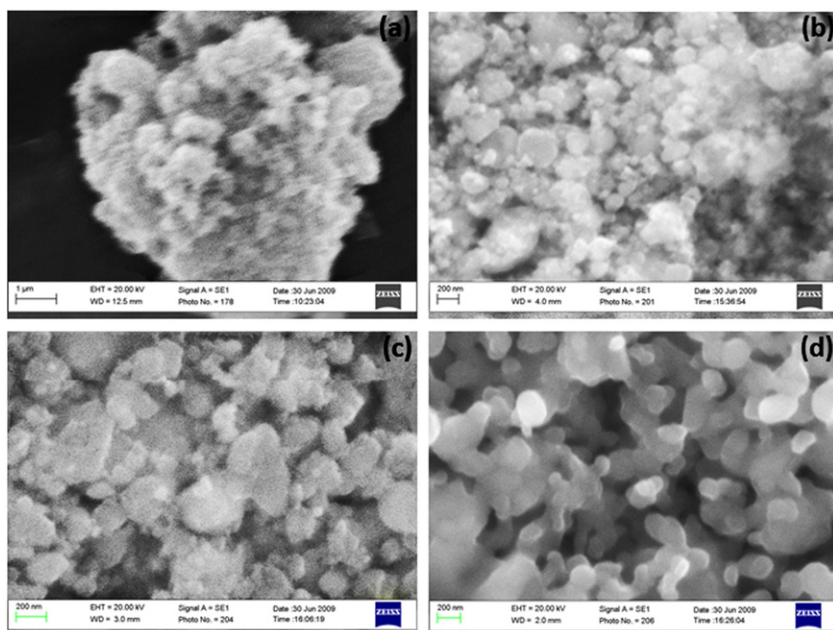


Fig. 1. Scanning Electron Micrographs of TiO<sub>2</sub>-Fe<sub>2</sub>O<sub>3</sub> oxide mixtures in the following conditions (a) as-milled, (b) annealing at 600 °C, (c) annealing at 750 °C, and (d) annealing at 1200 °C.

after annealing at 600 °C, respectively, one notes that there are no notable differences in the overall shapes. However, as the powder is further annealed to a higher temperature (750 °C) the average nanoparticles size seems to increase and the surface becomes smoother. Moreover, a closer look at the surface morphology after annealing shows an agglomeration of fine particles, which might be attributed to the presence of high surface energies attracting and eventually combining particles in the close vicinity [11]. As the powder is annealed up to 1200 °C, the particles appear to have fused together, forming links between them, which might be depicted from Fig. 1d). This is expected to be through melting of particle surfaces at temperatures below the melting point of their bulk form. A possible explanation for such a phenomenon is that in nano-phase materials a large fraction of atoms are present at the grain boundaries, which exhibit enhanced diffusivity and weak binding of the surface atoms, causing a sharp decrease of the surface melting point of the particles as the particle size reaches the nano-region [12]. A similar mechanism, based on solid state diffusion, has also been suggested by Nanda et al. [13] in accordance with the Oswald Ripening theory. Nanda et al. [13] has speculated that the increase in particle size with the increase in annealing temperature might be attributed to potential differences between small and large particles leading to the merging of the smaller particles into their larger counterparts. Hence, the nanostructure described above might be classified into two categories: (i) the first presented in the nanographs of the as-milled mixture (a), annealed at 600 °C (b), and annealed at 750 °C (c); ii) the second exhibited in the nanograph of the annealed oxide mixture at 1200 °C (d). In the nanographs of the first category one might readily notice the co-existence of oxide nanoparticles exhibiting similar structures, which are expected to belong to  $\text{Fe}_2\text{O}_3$  and to  $\text{TiO}_2$ . This observation might be supported by the XRD patterns generated for this particular category, in which the diffraction peaks belonging to  $\text{Fe}_2\text{O}_3$  and  $\text{TiO}_2$  phases were simultaneously detected. In the second category, i.e. annealing at 1200 °C, the SEM nanograph in Fig. 1d shows a new structure of nanoparticles with a smooth surface dominating the oxide mixture and different from the nanostructure described in nanographs of the first category, see Fig. 1a–c. These observations might be confirmed by the birth and subsequent growth of unprecedented peaks that differ from and overshadow in intensity those exhibited by the (category 1)  $\text{Fe}_2\text{O}_3$  and  $\text{TiO}_2$  individual peaks as annealing temperatures are increased beyond 900 °C. Moreover, during the preceding (category 1) lower temperature annealings the intensity ratios between major peaks in  $\text{Fe}_2\text{O}_3$  and  $\text{TiO}_2$  individual spectra were found to gradually increase in response to the rise in annealing temperatures. It is important to note that  $\text{Fe}_2\text{O}_3$  peaks were found larger than those of  $\text{TiO}_2$  and that the as-milled patterns were taken as a reference. This might indicate that the two oxides  $\text{Fe}_2\text{O}_3$  and  $\text{TiO}_2$  diffuse into each other forming a new phase. The patterns generated

for each category will be explored in further depth later in the context of discussing the XRD analysis results.

### 3.2. Structure evolution

X-ray diffraction (XRD) patterns of the as-received  $\alpha\text{-Fe}_2\text{O}_3$  phase within the hexagonal corundum-type structure (indexed as \*) and the as-received  $\text{TiO}_2$  phase with a rutile-type structure (indexed as +) are illustrated in Fig. 2. It is important to note the co-presence of a very small amount of anatase with a major peak (1 0 1) observed at 25° accompanying the main phase detected (rutile) in the XRD pattern for  $\text{TiO}_2$ . XRD pattern of the as-milled mixture (Fig. 3) reveals that  $\text{TiO}_2$  and  $\text{Fe}_2\text{O}_3$  diffraction peaks remain after milling with drastic broadening and decrease in the relative intensity due to the particle size reduction and accumulation of microstrains. The existence of peaks belonging to both  $\text{Fe}_2\text{O}_3$  and  $\text{TiO}_2$  phases confirm the above discussion of SEM results which indicates the coexistence of both oxides. Nonetheless, a

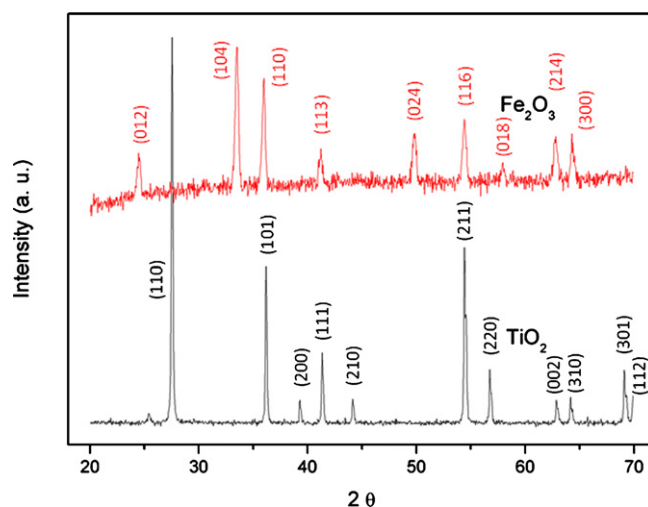


Fig. 2. XRD patterns of the as-received  $\text{Fe}_2\text{O}_3$  and  $\text{TiO}_2$  oxides.

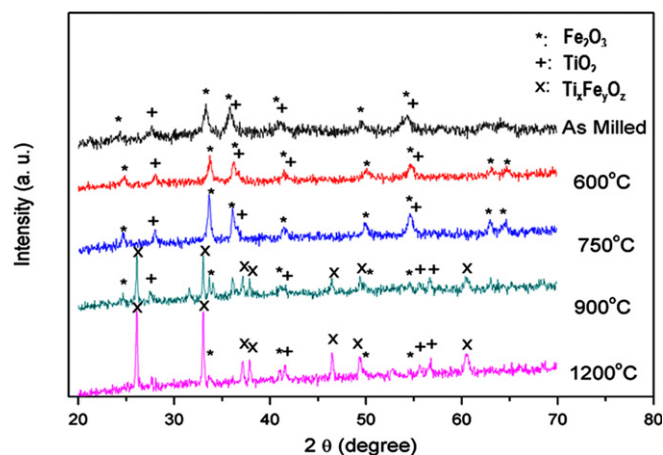


Fig. 3. XRD patterns of the as-milled and annealed  $\text{TiO}_2\text{-Fe}_2\text{O}_3$  mixtures.

careful examination of the patterns presented in Fig. 3 might lead to the conclusion that most of the peaks detected belong to the  $\text{Fe}_2\text{O}_3$  phase with slight remnants of the  $\text{TiO}_2$  phase. Moreover, it might be safe to argue that the anatase phase of  $\text{TiO}_2$  has been eliminated by mechanical milling. Fig. 3 illustrates the effect of annealing on the as-milled  $\text{Fe}_2\text{O}_3$ – $\text{TiO}_2$  mixture. After annealing at 600 °C, diffraction peaks of both phases are still apparent as predicted from SEM, with a slight increase in the relative intensity and a reduction in the peaks width suggesting an increase in the average crystallite size. This interdependency between XRD peak intensity/broadening and crystallite size was also demonstrated by Kasetsart et al. [14] for irregular polycrystalline  $\text{TiO}_2$ . Further heating to 750 °C did not cause any change in terms of phase formation, as it merely had the effect of further increasing the intensity whilst reducing the width of XRD peaks. This phenomenon was evident from the SEM nanographs where the particle size was indeed found to be correspondingly on the rise in response to the increase in annealing temperature from 600 to 750 °C. It is important to note that the intensity ratio between the major peaks of  $\text{Fe}_2\text{O}_3$  and  $\text{TiO}_2$  phases is constantly increasing relative to the as-milled mixture, suggesting a possible insertion of Ti atoms into  $\text{Fe}_2\text{O}_3$  crystal lattice thus reducing the intensity of  $\text{TiO}_2$  and thereby enhancing the peaks of  $\text{Fe}_2\text{O}_3$ . Nevertheless, heating has enhanced the rutile phase in agreement with the results reported by Pal et al. [6]. While He et al. [8] reported that  $\text{TiO}_2$  retain its anatase phase even after doping with  $\text{Fe}_3\text{O}_4$ . However, the insertion of Ti into

$\text{Fe}_2\text{O}_3$  crystal lattice reaches a critical state, whereby further annealing at 900 °C one observes the appearance of new sharp peaks with relatively high intensity (indexed by [1 1 0] and [2 0 3]) suggesting the formation of a new phase. By further annealing the oxides mixture at 1200 °C, the XRD pattern shows further enhancement of the intensities measured for the new peaks whereas major peaks belonging to both  $\text{Fe}_2\text{O}_3$  and  $\text{TiO}_2$  phases almost completely disappear. The new peaks represent an intermixture of  $\text{Fe}_2\text{O}_3$  and  $\text{TiO}_2$  oxides forming the new phase  $\text{Ti}_x\text{Fe}_y\text{O}_z$ . Through the consultation of Ti–Fe–O ternary phase diagrams and related literature [15–17], two phases, namely the spinel ( $\text{TiFe}_2\text{O}_4$ ) and Pseudobrookite ( $\text{TiFe}_2\text{O}_5$ ) phases might be nominated amongst those most thermodynamically likely to form (i.e. stable). However, it might be safe to speculate that the Pseudobrookite phase ( $\text{TiFe}_2\text{O}_5$ ) is what was indexed/ detected at 900–1200 °C as the emerging new phase, since diffraction peak indexing, intensities and corresponding angles measured for the new phase were found to be all in coincidence with corresponding peaks in available database [18,19]. The generation of the new phase is also supported by the corresponding SEM nanograph, where a seemingly new structure of relatively larger and interlinked nanoparticles exhibiting smooth surfaces dominates the oxide mixture.

### 3.3. Magnetic properties

Fig. 4 illustrates the hysteresis loop of VSM measurements for the as-received  $\text{TiO}_2$  and  $\text{Fe}_2\text{O}_3$  oxides. It is clear that both oxides are ferromagnetic, with  $\text{TiO}_2$  phase having a very low saturation magnetization ( $M_s$ ) value compared to that of  $\text{Fe}_2\text{O}_3$  phase, about 0.002 emu/g and 1.5 emu/g respectively. The as-milled mixture shows a ferromagnetic behavior (Fig. 4) with a saturation magnetization  $M_s$  higher than that of both pure starting phase, 2.6 emu/g which is almost twice that of pure  $\text{Fe}_2\text{O}_3$ , magnetic coercivity  $H_c=199$  Oe, and remanence magnetization  $M_r=0.378$  emu/g as illustrated in Table 1. He et al. [8] reported that  $\text{Fe}_3\text{O}_4$ : $\text{TiO}_2$  core-shell nanoparticles show superparamagnetic behavior with a coercivity of zero (0.0 Oe). This variance could be attributed to the fact that in the present work  $\text{Fe}_2\text{O}_3$  was used instead of  $\text{Fe}_3\text{O}_4$ . Furthermore, it could be also attributed to the phase of  $\text{TiO}_2$ , in the present work  $\text{TiO}_2$  rutile phase was used while He et al. [10] used anatase phase. However, as the mixture

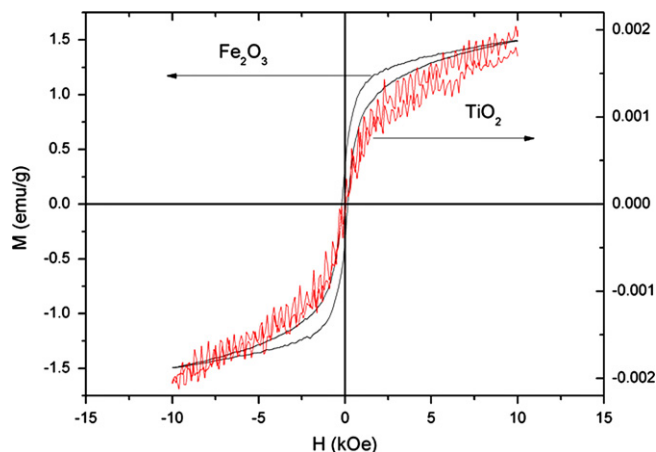


Fig. 4. VSM results of the as-received  $\text{Fe}_2\text{O}_3$  and  $\text{TiO}_2$  oxides.

Table 1

Structural parameters and magnetic properties for  $\text{TiO}_2$ – $\text{Fe}_2\text{O}_3$  oxide mixture in the as-milled and annealed at 750 °C conditions.

	CS (nm)	LS (%)	$H_c$ (Oe)	$M_r$ (emu/g)	$M_s$ (emu/g)
As-milled	20.9	0.709	195.7	0.405	2.93
600	27.3	0.564	160.1	0.223	1.81
750	35.5	0.46	157.9	0.1	1.0
900 (New phase)	59.1	0.26	116.5	0.0154	0.60
1200 (New phase)	156.8	0.216	293.2	0.00946	0.23



oxide was annealed at 600 °C and then at 750 °C the value of  $M_s$  decreased to 1.81 emu/g and 1.0 emu/g respectively, which is lower than that of pure  $\text{Fe}_2\text{O}_3$  phase, but maintaining a ferromagnetic behavior. This fact is a further evidence of the insertion of Ti atoms into  $\text{Fe}_2\text{O}_3$  crystal lattice, since  $\text{TiO}_2$  has a low saturation magnetization, therefore annealing enables some of Ti atoms to dissolve into the crystal lattice of  $\text{Fe}_2\text{O}_3$  (as observed in X-ray diffraction analysis), thus reducing  $M_s$  value even below that of  $\text{Fe}_2\text{O}_3$  since  $\text{TiO}_2$  shows a very weak magnetization (see Fig. 4). Remanence magnetization ( $M_r$ ) shows similar behavior with a drastic reduction in  $M_r$  value as the mixture oxide was annealed at 600 °C and 750 °C, while magnetic coercivity ( $H_c$ ) shows only a slight change, i.e. a reduction of about 19%. However, when the oxide mixture was annealed at 900 °C the ferromagnetic phase almost disappeared and a superparamagnetic phase take place instead as shown in Fig. 5 (with little trace of ferromagnetic phase can be seen in Fig. 6), which is

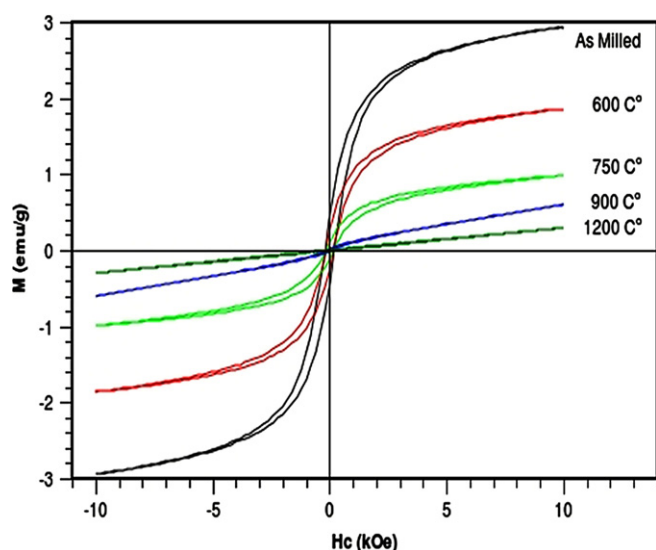


Fig. 5. VSM results of as-milled and annealed  $\text{TiO}_2\text{-Fe}_2\text{O}_3$  mixture.

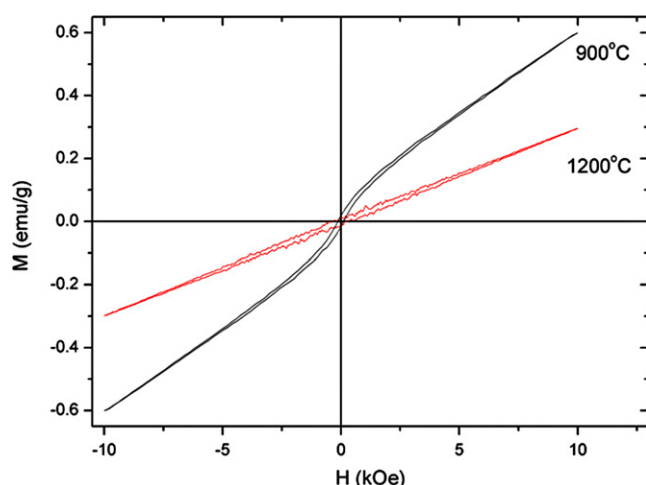


Fig. 6. VSM results for oxide mixture annealed at 900 °C and 1200 °C.

additional evident for a change of phase as previously was observed from SEM images and XRD patterns. The trace of ferromagnetic phase is due to a remaining of  $\text{Fe}_2\text{O}_3$  phase as observed in the XRD pattern. The biggest reduction was observed to be for  $M_r$ , with a reduction of almost one order of magnitude, and when the mixture annealed at 1200 °C  $M_r$  was further reduced by one order of magnitude with lower slope of magnetization than the slope at 900 °C. The increase in  $H_c$  for annealing at 1200 °C is due to the lower slope which can be noted by careful observation of Fig. 6.

#### 4. Conclusion

X-ray diffraction analysis of the milled mixture reveals that both oxides retain their structure followed by a very important peaks broadening due to the particle size reduction and accumulated strains. By annealing the oxide mixture, Ti atoms incorporate into  $\text{Fe}_2\text{O}_3$  crystal lattice and shows a ferromagnetic behavior until 750 °C. Annealing at 900 °C and 1200 °C shows a change in phase, this change in phase is evident from SEM images, XRD pattern, and VSM results. Moreover, VSM results show a reduction in value of the saturation magnetization as annealing increases but a drastic reduction in  $M_r$  was observed when annealing annealed at 900 °C and 1200 °C and transforming from ferromagnetic phase to paramagnetic phase. Thus annealing increases the insertion of Ti into  $\text{Fe}_2\text{O}_3$  crystal lattice until a critical density is reached and then a change of phase takes place.

#### References

- [1] P.A. Christensen, T.P. Curtis, T.A. Egerton, S.A.M. Kosa, J.R. Tinlin, Photoelectrocatalytic and photocatalytic disinfection of E. coli suspensions by titanium dioxide, *Applied Catalysis B: Environmental* 41 (2003) 371–386.
- [2] A.M.G.C. Dias, A. Hussain, A.S. Marcos, A.C.A. Roque, A biotechnological perspective on the application of iron oxide magnetic colloids modified with polysaccharides, *Biotechnology Advances* 29 (2011) 142–155.
- [3] K. Nomura, C.A. Barrero, J. Sakuma, M. Takeda, Room-temperature ferromagnetism of sol-gel-synthesized  $\text{Sn}_{1-x}\text{Fe}_x\text{O}_{2-\delta}$  powders, *Physical Review B* 75 (2007) 184411.
- [4] J. Sakuma, K. Nomura, C.A. Barrero, M. Takeda, Mössbauer studies and magnetic properties of  $\text{SnO}_2$  doped with  $^{57}\text{Fe}$ , *Thin Solid Films* 515 (2007) 8653–8655.
- [5] F. Gracia, J.P. Holgado, F. Yubero, A.R. Gonzalez-Eliphe, Phase mixing in  $\text{Fe}/\text{TiO}_2$  thin films prepared by ion beam-induced chemical vapour deposition: optical and structural properties, *Surface and Coating Technology* 158–159 (2002) 552–557.
- [6] B. Pal, M. Sharon, G. Nogami, Preparation and characterization of  $\text{TiO}_2/\text{Fe}_2\text{O}_3$  binary mixed oxides and its photocatalytic properties, *Materials Chemistry and Physics* 59 (1999) 254–261.
- [7] T.K. Kundu, M. Mukherjee, D. Chakravorty, T.P. Sinha, Growth of nano- $\alpha\text{-Fe}_2\text{O}_3$  in a titania matrix by the sol-gel route, *Journal of Materials Science* 33 (1998) 1759–1763.
- [8] Q. He, Z. Zhang, J. Xiong, Y. Xiong, H. Xiao, A novel biomaterial –  $\text{Fe}_3\text{O}_4/\text{TiO}_2$  core-shell nano particle with magnetic performance and high visible light photocatalytic activity, *Optical Materials* 31 (2008) 380–384.

- [9] P. Xiaoyan, J. dongmei, L. Yan, M. Xueming, Structural characterization and ferromagnetic behavior of Fe-doped  $\text{TiO}_2$  powder by high-energy ball milling, *Journal of Magnetism and Magnetic Materials* 305 (2006) 388–391.
- [10] A. Al-Saie, S. Arekat, A. Jaafar, M. Bououdina, Synthesis, structure and magnetic properties of nano-sized  $\text{CoFe}_2\text{O}_4$  material, *International Journal of Nanoparticles* 2 (2009) 507–511.
- [11] S.A. Ibrahim, S. Sreekantan, Effect of annealing atmosphere towards  $\text{TiO}_2$  nanoparticles on their photocatalytic performance in aqueous phase, in: *Proceedings of International Conference on Enabling Science and Nanotechnology (ESciNano)* (2010) KLCC, Malaysia.
- [12] V. Kumar, A. Rana, M.S. Yadav, R.P. Pant, Size-induced effect on nano-crystalline  $\text{CoFe}_2\text{O}_4$ , *Journal of Magnetism and Magnetic Materials* 320 (2008) 1729–1734.
- [13] K.K. Nanda, F.E. Kruis, H. Fissan, Evaporation of free PbS nanoparticles: evidence of the Kelvin effect, *Physical Review Letters* 89 (2002) 256103.
- [14] K. Thamaphat, P. Limsuwan, B. Ngotawornchai, Phase characterization of  $\text{TiO}_2$  powder by XRD and TEM, *Kasetsart Journal (Natural Science)* 42 (2008) 357–361.
- [15] C. Franke, G.M. Pennock, M.R. Drury, R. Engelmann, D. Lattard, J.F.L. Garming, T. von Döbeneck, M.J. Dekkers, Identification of magnetic Fe–Ti oxides in marine sediments by electron backscatter diffraction in scanning electron microscopy, *Geophysical Journal International* 170 (2007) 545–555.
- [16] M. Gueguin, F. Cardarelli, Chemistry and mineralogy of titania-rich slags. Part 1 – hemo-ilmenite, sulphate and upgraded titania slags, *Mineral. Processing and Extractive Metallurgy Review* 28 (2007) 1–58.
- [17] H. Elstad, J.M. Eriksen, A. Hildal, T. Rosenqvist, S. Seim, Equilibrium between titania slags and metallic iron, in: *Proceedings of the Sixth International Heavy Minerals Conference ‘Back to Basics’*, The Southern African Institute of Mining and Metallurgy, 2007.
- [18] W. Yu-ming, Y. Zhang-fu, G. Zhan-cheng, T. Qiang-qiang, L. Zhao-yi, J. Wei-zhong, Reduction mechanism of natural ilmenite with graphite, *Transactions of Nonferrous Metals Society of China* 18 (2008) 962–968.
- [19] J. Morales, L. Sánchez, F. Martín, F. Berry, X. Ren, Synthesis and characterization of nanometric iron and iron-titanium oxides by mechanical milling: electrochemical properties as anodic materials in lithium cells, *Journal of Electrochemical Society* 152/9 (2005) A1748–A1754.